Alzheimer brains, astrocytes are stained for FGF-1 more strongly than those in control brains in both gray and white matters [52].

FGF-1 binds with all receptor isoforms such as FGF receptor 1 (FGFR1), FGFR2, FGFR3 and FGFR4 [47]. FGF-1 is likely synthesized and localized in the cytosol and nucleus of the producing cells, because it has no amino-terminal signal sequence for secretion as well as FGF-2 [39,57]. There is a report that disruption of endoplasmic reticulum (ER)-Golgi communication by brefeldin A has no effect on FGF-1 release from the producing cells [5], suggesting that the FGF-1 release to extracellular space is unlikely to be mediated by the classical intracellular transport system through the ER/Golgi pathway after the biosynthesis. The mechanism of FGF-1 release is unclear at present in spite of many previous investigations. We found that astrocytes enhance the production and release of FGF-under (acidic FGF, heparin-binding growth factor 1, HBGF-1) stressful condition such as long-term culture and cryoinjury [23,44,49,53]. FGF-1 enhances apoE/HDL generation of astrocytes accompanied by the up-regulation of syntheses of apoE and cholesterol in the autocrine or paracrine manner [24,44].

1. HDL Generation Mediated by Endogenous apoE and Exogenous apoA-I in Astrocytes

Human apoE composed of 299 amino acid residues is a glycoprotein with molecular weight of 37 kDa. ApoE is produced and secreted by many kinds of cells such as macrophages, steroid-producing cells, liver and small intestine in the peripheral tissues. In the CNS, apoE is mainly produced by astrocytes and partly by microglias [12]. The production of apoE is enhanced accompanied with brain development or regeneration of injured neurons [48]. Astrocytes secreted apoE along with cellular cholesterol and phospholipids as apoE/HDL particles with 10 – 17 nm in diameter. Astrocytes secrete apoJ also as smaller HDL (7.5 – 12 nm in diameter).

The mechanism of apoE secretion from astrocytes is unclear at present. We studied the mechanism of apoE secretion by using astrocytes prepared from fetal rat brain. Here, we describe regarding the mechanism for apoE secretion and apoE/HDL generation in astrocytes on the base of unpublished recent our data. The secretion of ^{35}S-labeled apoE started within 30 min in rat astrocytes. At 10 min after the start of metabolic biosynthesis of apoE with ^{35}S-methionine, ^{35}S-apoE was collected from the intracellular membrane fraction containing mainly lipid raft domain, suggesting that the intracellular apoE associates with lipid raft in the inside of Golgi apparatus or endosome in the process of intracellular transport of apoE. The apoE was secreted from wild-type mouse as apoE/HDL particles with density of 1.08 – 1.12 g/mL, while the astrocytes prepared from ATP-binding cassette transporter A1-deficient (ABCA1-KO) mouse secreted apoE as insufficiently lipidated HDL with higher density (d = 1.12 – 1.17 g/mL) into the conditioned medium. The intracellular apoE in ABCA1-KO astrocytes was collected from the non-lipid raft with higher density unlike that in wild type astrocytes (unpublished data), suggesting that ABCA1 is necessary to translocate apoE onto lipid raft for generation of mature HDL. This result has been confirmed by the different culture system using rat astrocytoma GA-1 cells, which express very low level of mRNAs of apoE and ABCA1 [22]. In rat apoE-transfected GA-1 cells (GA-1/25), the secreted apoE was

recovered with the HDL fractions with higher density similarly to the apoE secreted from ABCA1-KO astrocytes. When GA-1/25 cells were treated with TO901317, a LXR agonist, the cellular level of ABCA1 was increased in GA-1/25 cells. The intracellular apoE, furthermore, was increased in the membrane lipid raft fraction along with ABCA1 and the secreted apoE was collected from the apoE-HDL fraction with lower density as mature apoE/HDL. TO901317 failed to translocate ABCA1 to the lipid raft in GA-1/Mock cells without apoE, although the cellular ABCA1 level was increased in the non-raft domain but not the lipid raft by TO901317. This suggests that high lipidation of apoE for mature apoE/HDL generation is dependent on the enhancement of cellular ABCA1 level and the interaction between apoE and ABCA1 in the lipid raft domain. The membrane-associated apoE, indeed, was precipitated by an anti-ABCA1 antibody through ABCA1, and ABCA1 was also done by using an anti-apoE antibody, even after the cell surface ABCA1 and apoE were digested by the treatment with exogenously added trypsin. Although ABCA1 is generally thought to be distributed in non-lipid raft fraction, the astrocyte's ABCA1 appears to be localized in membrane lipid raft through the interaction with endogenous apoE.

Exogenously added human apoE generates apoE/HDL using both newly synthesized and pre-synthesized cholesterol through the interaction with the cell surface of astrocytes. Surprisingly, the endogenous apoE secreted from rat astrocytes used pre-synthesized cholesterol rather than newly synthesized one for apoE/HDL generation. This implies that the endogenous apoE in astrocytes exports preferentially the pre-synthesized cellular cholesterol to the conditioned medium. If apoE is secreted by astrocytes as a lipid-free apolipoprotein, the endogenous apoE must transport both newly synthesized and presynthesized cholesterol to the extracellular space like exogenously added apoE. Whether the apoE secreted from astrocytes is lipidated in intracellular site is very important issue to be addressed.

The mechanism for apoE secretion has been investigated mainly by using macrophages. After the biosynthesis in the endoplasmic reticulum, some of apoE molecules are likely secreted from the plasma membrane through O-linked glycosylation in the Golgi, while other large parts of apoE are digested in the lysosome [58]. In macrophages, the secreted apoE is re-internalized for the generation of apoE-HDL [59]. ApoE appears to be secreted from macrophages to rely on the functions of protein kinase A and microtubules via calcium-dependent pathway [31]. ABCA1 must participate greatly in apoE secretion, as deficiency of ABCA1 causes the decrease of apoE secretion [17,56].

On the other hand, apoA-I is reportedly produced by brain capillary endothelial cells [42]. Exogenous apoA-I generates phospholipids-rich and cholesterol-poor HDL through the interaction with ABCA1 in the non-lipid raft fraction of astrocytes as well as many kinds of peripheral cells and unlike the case of endogenous apoE in astrocytes [22]. We found a cytosolic lipid-protein particle (CLPP), defined as a lipid-protein complex with density of 1.09 - 1.16 g/ml and diameter 17 - 18 nm like plasma HDL in the cytosol fraction of rat astrocytes [21,25]. The CLPP participates in the intracellular cholesterol trafficking in association with apoA-I-mediated HDL generation. Caveolin-1, protein kinase Cα and cyclophilin A are recovered in the CLPP fraction after the stimulation of astrocytes with apoA-I [19,20]. The apoA-I-mediated cholesterol release is inhibited by cyclosporin A, an inhibitor of cyclophilin A. ApoA-I induces the tyrosine phosphorylation of phospholipase Cγ (PL-Cγ), followed by the translocation of PL-Cγ to the CLPP fraction and diacylglyceride production in the CLPP. The translocation and activation of protein kinase Cα to/in the CLPP

are continuously enhanced [29]. The suppression of either phospholipase C or protein kinase C inhibits apoA-I-mediated cholesterol release and apoA-I/HDL generation. These results suggest that the CLPP is an intracellular site of apoA-I-induced signal transduction and has a role as an intracellular cholesterol transporter. The different type of lipoproteins generated by apoE and apo A-I may exhibit different function in the brain [26].

2. Regulation by FGF-1 of apoE/HDL Generation

It is an interesting issue whether the apoE/HDL generation by astrocytes is regulated dependently on cellular cholesterol level of astrocytes or controlled by the unknown system to detect cholesterol level in the brain. We found that some trophic factor is one of regulators for apoE/HDL generation under the stressful conditions. Rat astrocytes enhance syntheses of cholesterol and apoE, resulted in increasing generation of apoE/HDL during long-term culture [23]. The mRNA expression and production of FGF-1 are also increased in rat astrocytes cultured over three weeks. FGF-1 enhances biosyntheses of apoE and cholesterol by an autocrine or paracrine fashion, leading to an enhanced generation of apoE/HDL.

The cholesterol synthesis was enhanced through the phosphorylations of MEK and ERK in rat astrocytes stimulated with FGF-1, implying the dependency of cholesterol synthesis on activation of MAP kinase cascade [24]. In apoE-deficient (apoE-KO) mouse astrocytes, FGF-1 stimulates cholesterol biosynthesis without enhancing its release, indicating a pathway independent of apoE secretion [24]. LY294002, an inhibitor of phosphatidylinositide 3-OH kinase (PI3K), suppressed not only Akt phosphorylation but also apoE secretion and apoE/HDL generation without suppression of cholesterol biosynthesis.

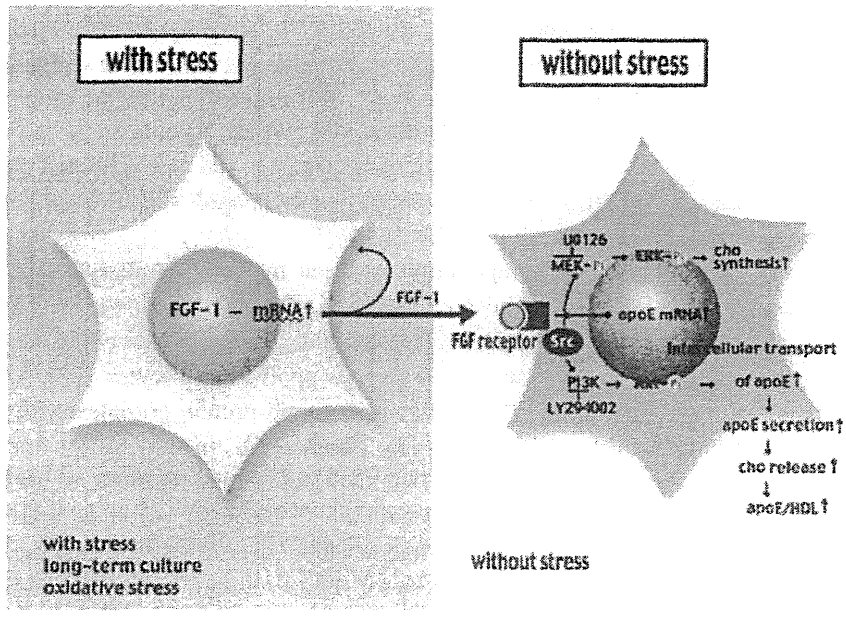

Figure 1. Mechanism of apoE/HDL generation by FGF-1 in rat astrocytes.

This cell signaling and apoE/HDL generation mediated by FGF-1 were suppressed by the inhibition of Src activity [46]. The increase by FGF-1 of apoE mRNA expression is not influenced by either LY294002 or U0126, a MEK inhibitor, in rat astrocytes. Interestingly, the apoE secretion from GA-1/25 cells was increased by FGF-1 and reversed by LY294002, despite of the lack of effect of FGF-1 and LY294002 on the apoE transcription step. As the change of apoE level in the medium and cell is reciprocal, the effect of FGF-1 seems to be on the process of apoE transport/secretion through the activation of PI3K rather than its translation.

FGF-1 increases mRNA expression of liver X receptor α (LXRα) in addition to apoE in rat astrocytes. Increase of LXRα is suppressed by inhibition of the FGF receptor-1 and MEK/ERK but not by inhibition of PI3K/Akt [37]. The liver X receptor element responsible for activation of the rat apoE promoter by FGF-1 is located between -450 and -320bp, and the direct repeat 4 (DR4) element in this region (-448 to -433bp) is responsible for the activation. It was demonstrated by Chromatin immunoprecipitation analysis that FGF-1 enhances association of LXR with the rat apoE promoter. FGF-1 also enhances biosynthesis of LXR ligand, such as 25-hydroxycholesterol. Thus, FGF-1 enhances apoE/HDL generation through at least three different signal transductions in astrocytes (Figure 1).

3. FGF-1 Release from Astrocytes

Rat astrocytes increase the production and release of FGF-1 to enhance apoE/HDL generation under the long-term culture stress and cryo-injury, suggesting that FGF-1 functions as a regulator of apoE/HDL production to contribute to recovery of the brain from damage. We therefore attempted to search a trigger to induce the synthesis and release of FGF-1 in astrocytes under stress conditions to understand regulation system of apoE/HDL generation in the brain. Oxidative stress is one of the common events in the case of brain damage. The release of FGF-1 was enhanced along with cytosolic proteins such as HSP70, HSP90, PK-Cδ and β–actin from both conventional and long-term cultured rat astrocytes by the treatment with 100 μM H_2O_2 without inducing apoptosis in the cells. Hydrogen peroxide, furthermore, increased the permeation of membrane-nonpermeable molecules such as Rhodamine-phalloidin and trypsin into rat astrocytes. The release of [^{35}S]-labeled cytosolic proteins with a wide range of molecular weight was increased by the treatment with H_2O_2 from rat astrocytes, after metabolical labeling with [^{35}S]-methionine. These findings suggest that the release of FGF-1 from astrocytes treated with H_2O_2 is hardly mediated by the mechanism specific to FGF-1 molecule. The hydrogen peroxide-mediated release of cytosolic proteins is suppressed by the treatment with antioxidants. As FGF-1 has no biochemical activity to rat astrocytes damaged with H_2O_2, the FGF-1 released from H_2O_2–treated astrocytes is thought to act much more on healthy astrocytes without stress or injury in the manner of paracrine than on damaged astrocytes in autocrine action. The healthy astrocytes stimulated with FGF-1 are able to produce actively apoE/HDL through the enhancement of biosyntheses and release of apoE and cholesterol. Astrocytes are more sensitive to H_2O_2 than cell lines such as bovine endothelial cells and HepG2 cells for release of cytosolic proteins. Higher sensitivity of astrocytes to oxidative stress may be effective to protect the brain against oxidative stress by using the released FGF-1.

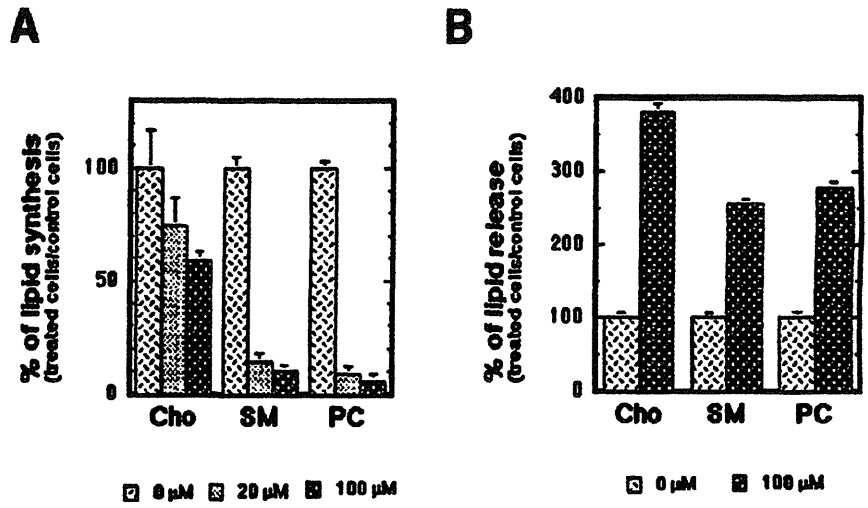

Figure 2. Effects of H2O2 on lipid synthesis and relese in rat astrocytes.

Hydrogen peroxide suppresses transiently biosyntheses of lipids such as cholesterol, phosphatidylcholine and sphingomyelin and enhances lipid release in/from astrocytes (Figure 2). This imply that oxidative stress lowers membrane lipid content of astrocytes by suppression of lipid synthesis and increase in lipid release, makes the membrane unstable and increases membrane-permeability for the release of FGF-1 along with cytosolic proteins. Interestingly, the lipid synthesis of HepG2 and endothelial cells is suppressed by H_2O_2 much less than that of astrocytes. Such findings lead us to the speculation that the sensitive reactivity to oxidative stress for FGF-1 release may be one of important functions of astrocytes to protect the brain against oxidative stress. FGF-1 appears to be localized in the neural tissue as a high molecular weight complex. The complex contains FGF-1 and p40 extravasecular domain of synaptotagmin (Syn)-1, and the brain-derived FGF-1/p40 Syn-1 complex is found associated with the calcium-binding protein, S100A13 [2,34]. FGF-1 is released as a latent homodimer with the p40 extravasecular domain of synaptotagmin (Syn)-1 by heat-shock stress. These reports exhibit that FGF-1 is released as complex forms under the stress conditions, though the biochemical significance of FGF-1/synaptotagmin-1 complex is unclear for FGF-1 release at present.

4. Brain Protection from Injury and Stress by FGF-1 and apoE/HDL

There have been abundantly reported that the apoE/HDL produced by astrocytes participates in development of the CNS to promote synaptogenesis, neurite outgrowth and axon growth [6,11]. ApoE production is dramatically increased in the brain after injury of the rat sciatic and optic nerves [48]. Nerve injury has been observed to stimulate the secretion of apoE by glial cells. With respect to the role(s) of apoE/HDL in the brain injury, apoE reportedly protects against oxidative stress by reducing glutamate toxicity [35]. H. Hayashi et al. reported that apoE/HDL protects neurons from apoptosis through activation of

phospholipase Cγ1 and inhibition of calcineurin mediated by LDL receptor-related protein-1 [14,15]. These lines of evidence suggest that the apoE/HDL derived from astrocytes contributes to maintain viability and function of neurons, and protect neuronal cells from stress and injury in the CNS. Thus, why and how apoE/HDL production is enhanced by injury of the brain would be a critical question to be addressed.

It has been well known that FGF-1 is released in response to sublethal cell injury such as oxidative stress, heat shock, hypoxia and serum starvation. The production of FGF-1 has been demonstrated immunohistochemically in the post-injury reactive astrocytes of mice in vivo [45]. FGF-1 is highly expressed in motor neurons and released in response to oxidative stress [3]. Even NIH 3T3 cells transfected with a synthetic gene encoding FGF-1, secrete FGF-1 into the conditioned medium when these cells are exposed to heat shock (at 42 °C for 2 h), but not under the regular conditions at 37 °C [27]. FGF-1 is apparently produced and released in/from astrocytes in response to exposure to stress and injury in the brain. We demonstrated that the productions of FGF-1 and apoE are increased in the astrocytes around the lesion of cryo-injury in the mouse brain [49]. The FGF-1 production was ahead of the increase of apoE synthesis and the wound healing was substantially delayed in the apoE-deficient mice. The production of FGF-1 was obviously increased in the injured brain of apoE-deficient mouse also. These findings imply that cryo-injury promotes astrocytes to produce and secrete FGF-1, which up-regulates the apoE/HDL generation to assists wound healing. In neurodegenerative diseases including Alzheimer's disease, it is known that there is ongoing neuronal damage, inflammation, or generation of oxidative stress, implaying that FGF-1 release may be enhanced in the brain of patients with AD [52]. On the base of these findings, it may be possible to postulate that stress and injury enhance FGF-1 release from astrocytes and the released FGF-1 acts on the healthy astrocytes in the manner of paracrine action to increase the production of apoE/HDL for protection and recovery of neural cells from stress and injury in the brain.

5. Production and Function of FGF-1 and apoE/lipoproteins in Alzheimar's Desease

Because production of FGF-1 is enhanced by the injury or oxidative stress, it is reasonable to assume that its expression level is upregulated in neurodegenerative diseases including Alzheimer disease (AD). It has been reported that FGF-1 expression level is increased in reactive astrocytes surrounding senile plaques and the distribution pattern of FGF-1 receptor shows a similar to that of FGF-1 [50]. FGF-1 expression level in entorhinal cortex is likely decreased in AD brains compared with control cases, while remaining neurons showed significantly higher at FGF-1 immnoreactivity [51], suggesting that not only astrocytes, but also neurons express FGF-1 to protect themselves in the brain. In addition to expression of FGF-1 in human brains, it has been shown that the levels of FGF-1 in the CSF and serum from the patients with AD was significantly higher than in patients without AD [38]. Taken all these results together, it may be possible that in the surrounding area of damaged brain region caused by Aβ deposition in AD brain, astrocytes and some types of neurons enhance synthesis and release of FGF-1, which up-regulates syntheses of apoE and cholesterol leading to enhance generation of apoE/HDL for neuronal repair and protection.

With respect to roles of apoE or cholesterol in AD pathogenesis, it has been reported that cholesterol level in the CSF of patients with AD is decreased compared with those with non-AD disease [7,43]. The major part of cholesterol in the CSF exists as a component of HDL, which is generated by apoE derived from astrocytes in an apoE-isoform-dependent manner [13,40,41]. The generation of HDL by apoE3 is greater than apoE4. Because ABCA1 is a key molecule for apoE-mediated HDL generation to maintain adequate cholesterol homeostasis and distribution, ABCA1 has gained attention as being an important protein target for both AD pathogenesis and treatment.

There are several studies showing that ABCA1 deletion leads to an increase in both amyloid β (Aβ) and amyloid burden in the brains of transgenic mouse models [16,32,54], although ABCA1 deletion did not alter Aβ production [54]. It has been demonstrated that the fully lipidated apoE/HDL was required for Aβ degradation in microglia, indicating that the presence of ABCA1 and subsequent formation of apoE/HDL have an effect on Aβ clearance [28]. The effect of ABCA1 and HDL generation on Aβ clearance has been confirmed by a study using ABCA1 transgenic mice, showing that there was a dramatic decrease in the amount of Aβ deposition [55]. Based on these data, it is possible that the regulation of apoE/HDL level via ABCA1 may be targets for development AD therapies. In addition, because FGF-1 is known to stimulate synthesis of apoE, cholesterol, and phospholipids, leading to increased generation of apoE/HDL, modulation of FGF-1 may be an alterative target for AD therapy.

References

[1] Bjorkhem, i. and Meaney, S., Brain cholesterol: long secret life behind a barrier, *Arterioscler. Thromb. Vasc. Biol.*, 24 (2004) 806-815.

[2] Carreira, C.M., LaVallee, T.M., Tarantini, F., Jackson, A., Lathrop, J.T., Hampton, B., Burgess, W.H. and Maciag, T., S100A13 is involved in the regulation of fibroblast growth factor-1 and P40 synaptotagmin-1 release in vitro, *J. Biol. Chem.*, 273 (1998) 22224-22231.

[3] Cassiana, P., peher, M., Vargas, M.R., Castellanos, R., Barbeito, A.G., Estevez, A.G., Thompson, J.A. and Beckman, J.S., Astrocyte activation by fibroblast growth factor-1 and motor neuron apoptosis: implications for amyotrophic lateral sclerosis, *J. Neurochem.*, 93 (2005) 38-46.

[4] Chiba, H., Mitamura, T., Fujisawa, S.-i., Ogata, A., Aimoto, Y., Tashiro, K. and Kobayashi, K., Apolipoproteins in rat cerebrospinal fluid: a comparison with plasma lipoprotein metabolism and effect of aging, *Neurosci. Letters*, 133 (1991) 207-210.

[5] Christofori, G. and Luef, S., Novel forms od acidic fibroblast growth factor-1are constitutively exported by beta tumor cell lines independent from conventional secretion and apoptosis, *angiogenesis*, 1 (1997) 55-70.

[6] DeMattos, R.B., Curtiss, L.K. and L., W.D., A minimally lipidated form of cell-derived apolipoprotein E exhibits isoform-specific stimulation of neurite outgrowth in the absence of exogenous lipids or lipoproteins, *J. Biol. Chem.*, 273 (1998) 4206-4212.

[7] Demeester, N., Castro, G., Desrumaux, C., De Geitere, C., Fruchart, J.-C., santens, P., Mulleners, E., Engelborghs, S., De Deyn, P.P. and Vandekerckhove, J.,

Characterization and functional studies of lipoproteins, lipid transfer proteins, and lecithin:cholesterol acyltransferase in CSF of normal individuals and patients with Alzheimer's disease, *L. Lipid res.*, 41 (200) 963-974.

[8] Dono, R., Fibloblast growth factors as regulators of central nervous system development and function, *Am. J. Physiol. Regul. Integr. Comp. Physiol.*, 284 (2003) R876-R881.

[9] Eckenstein, F.P., Andersson, C., Kuzis, K. and Woodward, W.G., Distribution of acidic and basic fibroblast growth factors in the mature, injured and developing rat nervous sysem, *Progress Brain Res.*, 103 (1994) 55-63.

[10] Exkenstien, F.P., Fibloblast growth factors in the nervous system, *J. Neurobiol.*, 25 (1994) 1467-1480.

[11] Fagan, A.M., Bu, G., Sun, Y., Daugherty, A. and Holtzman, D.M., Apolipoprotein E-containing high density lipoprotein promotes neurite outgrowth and is a ligand for the low density lipoprotein receptor-related protein, *J. Biol. Chem.*, 271 (1996) 30121-30125.

[12] Fujita, S.C., Sakuta, K., Tsuchiya, R. and Hamamaka, H., Apolipoprotein E is found in astrocytes but not in microglia in the normal mouse brain, *Neurosci. Res.*, 35 (1999) 123-133.

[13] Gong, J.-S., Kobayashi, M., Hayashi, H., Zou, K., Sawamura, N., Fujita, S.C., Yanagisawa, K. and Michikawa, M., Apolipoprotein E (ApoE) isoform-dependent lipid release from astrocytes prepared from human ApoE3 and ApoE4 knock in mice, *J. Biol. Chem.*, 277 (2002) 29919-29926.

[14] Hayashi, H., Campenot, R.B., Vance, D.E. and E., V.J., Apolipoprotein E-containing lipoproteins protect neurons from apoptosis via signaling pathway involving low-density lipoprotein receptor-related protein-1, *J. Neurosci.*, 27 (2007) 1933-1941.

[15] Hayashi, H., Campenot, R.B., Vance, D.E. and Vance, J.E., Glial lipoproteins stimulate axon growth of central nervous system neurons in compartmented cultures, *J. Biol. Chem.*, 279 (2004) 14009-14015.

[16] Hirsch-Reinshagen, V., Maia, L.F., Burgess, B.L., Blain, J.F., Naus, K.E., McIsaac, S.A., Parkinson, P.E., Chan, J.Y., Tansley, G.H. and Hayden, M.R., The absence of ABCA1 decreases soluble ApoE levels but does not diminish amyloid deposition in two murine models of Alzheimer disease, *J. Biol. Chem.*, 280 (2005) 43243-43256.

[17] Hirsch-Reinshagen, V., Zhou, S., Burgess, B.L., Bernier, L., Hayden, M.R. and Wellington, C.L., Deficiency of ABCA1 impairs apolipoprotein E metabolism in brain, *J. Biol. Chem.*, 279 (2004) 41197-41207.

[18] Hossain, W.A. and Morest, D.K., Fibroblast grwth factors (FGF-1, FGF-2) promote migration and neurite growth of mouse cocchlear ganglion cells in vitro: immunohistochemistry and antibody perturbation, *J. Neurosci. res.*, 62 (2000) 40-55.

[19] Ito, J.-i., Kheirollah, A., Nagayasu, Y., Lu, R., Kato, K. and Yokoyama, S., Apolipoprotein A-I increases association of cytosolic cholesterol and caveolin-1 with microtubule cytoskeletons in rat astrocytes., *J. Neurochem.*, 97 (2006) 1034-1043.

[20] Ito, J.-i., Li, H., Nagayasu, Y., Kheirollah, A. and Yokoyama, S., Apolipoprotein A-I induces translocation of protein kinase Calpha to a cytosolic lipid-protein particle in astrocytes, *J. Lipid Res.*, 45 (2004) 2269-2276.

[21] Ito, J.-i., Nagayasu, Y., Kato, K., sato, R. and Yokoyama, S., Apolipoprotein A-I induces translocation of cholesterol, phospholipid, and caveolin-1 to cytosol in rat astrocytes. *J. Biol. Chem., Vol. 277*, 2002a, pp. 7929-7935.

[22] Ito, J.-i., Nagayasu, Y., Kheirollah, A., Abe-Dohmae, S. and Yokoyama, S., ApoA-I enhances generation of HDL-like lipoproteins through interaction between ABCA1 and phospholipase Cgamma in rat strocytes, *Biochim. Biophys. Acta*, 1811 (2011) 1062-1069.

[23] Ito, J.-i., Nagayasu, Y., Lu, R., Kheirollah, A., Hayashi, M. and Yokoyama, S., Astrocytes produce and secrete FGF-1, which promotes the production of apoE-HDL in a manner of autocrine action, *J. Lipid Res.*, 46 (2005) 679-686.

[24] Ito, J.-i., Nagayasu, Y., Okumura-Noji, K., Lu, R., Nishida, T., Miura, Y., Asai, K., Kheirollah, A., Nakaya, S. and Yokoyama, S., Mechanism for FGF-1 to regulate biogenesis of apoE-HDL in astrocytes., *J. Lipid Res.*, 48 (2007) 2020-2027.

[25] Ito, J.-i., Nagayasu, Y., Ueno, S. and Yokoyama, S., Apolipoprotein-mediated cellular lipid release requires replenishment of sphingomyelin in a phosphatidylcholine-specific phospholipase C-dependent manner, *J. Biol. Chem.*, 277 (2002b) 44709-44714.

[26] Ito, J.-i., Zhang, L.-Y., Asai, M. and Yokoyama, S., Differential generation of high-density lipoprotein by endogenous and exogenous apolipoproteins in cultured fetal rat astrocytes, *J. Neurochem.*, 72 (1999) 2362-2369.

[27] Jackson, A., Friedman, S., Zhan, X., Engleka, K.A., Forough, R. and Maciag, T., Heat shock induces the release of fibroblast growth factor 1 from NIH3T3 cells, *Proc. Natl. Acad. Sci. U. S. A.*, 89 (1992) 10691-10695.

[28] Jiang, Q., Lee, C.Y., Mandrekr, S., Wilkinson, B., Cramer, P., Zelcer, N., mann, K., Lamb, B., Wilkinson, B., Cramer, P., Zelcer, N., Mann, K., Lamb, B., Willson, T.M. and Collins, J.L., ApoE promotes the proteolytic degradation of Abeta, *Neuron*, 58 (2008) 681-693.

[29] Kheirollah, A., Ito, J.-i., Nagayasu, Y., Lu, R. and Yokoyama, S., Cyclosporin A inhibits apolipoprotein A-I-induced early events in cellular cholesterol homeostasis in rat astrocytes., *Neuropharmacol.*, 51 (2006) 693-700.

[30] Koch, S., Donarski, N., Goetze, K., Kreckel, M., Stuerenburg, H.-J., Buhmann, C. and Beisiegel, U., Characterization of four lipoprotein classes in human cerebrospinal fluid, *J. Lipid. Res.*, 42 (2001) 1143-1151.

[31] Kockx, M., Guo, D.L., Huby, T., Lesnik, P., Kay, J., Sabarentnam, T., Jary, E., Hill, M., Gaus, K., Chapman, J., Stow, J.L., Jessup, W. and Kritharides, L., Secretion of apolipoprotein E from macrophages occurs via a protein kinase A-and calcium-dependent pathway along the microtubule network, *Circulation Res.*, 101 (2007) 607-616.

[32] Koldamova, R., Staufenbiel, M. and Lefterov, I., Lack of ABCA1 considerably decreases brain ApoE level and increases amyloid deposition in APP23 mice, *J. Biol. Chem.*, 280 (2005) 43224-43235.

[33] Larsson, H., Klint, P., Landgren, E. and Claesson-Welsh, L., Fibroblast growth factor receptor-1-mediated endothelial cell proliferation is dependent on the Src homology (SH)2/SH3 domain-containing adaptor protein Crk., *J. Biol. Chem.*, 274 (1999) 25726-25734.

[34] LaVallee, T.M., Tarantini, F., Gamble, S., Carreira, C.M., Jackson, A. and Maciag, T., Synaptotagmin-1 is required for fibroblast growth factor-1 release, *J. Biol. Chem.*, 273 (1998) 22217-22223.

[35] Lee, Y., Aono, M., Laskowitz, D., Warner, D.S. and Pearistein, R.D., Apolipoprotein E protects against oxidative stress in mixed neuronal-glial cell cultures by reducing glutamate toxicity, *Neurochem. Int.*, 44 (2004) 107-118.

[36] Linton, M.F., Gish, R., Hubl, S.T., Butler, E., Esquivel, C., Bry, W.L., Boyles, J.K., Wardell, M.R. and Young, S.G., Phenotypes of apolipoprotein B and E after liver transplantation., *J. Clin. Invest.*, 88 (1991) 270-281.

[37] Lu, R., Ito, J.-i., Iwamoto, N., Nishimaki-Mogami, T. and Yokoyama, S., FGF-1 induces expression of LXR and production of 25-hydroxycholesterol to upregulate the apoE gene in rat astrocytes, *J. Lipid Res.*, in press (2009).

[38] Mashayekhi, F., Hadavi, M., Vaziri, H.R. and Naji, M., Increased acidic fibroblast growth factor concentrations in the serum and cerebrospinal fluid of patients with Alzheimer's disease., *J. Clin. Neurosci.*, 17 (2010) 357-359.

[39] Mason, I.J., The ins and outs of fibroblast growth factors, *Cell*, 78 (1994) 547-552.

[40] Michikawa, M. and Yanagisawa, K., Apolipoprotein E4 induces neuronal cell death under conditions of suppressed de novo cholesterol synthesis., *J. Neurosci. Res.*, 54 (1998) 58-67.

[41] Minagawa, H., Gong, J.-S., Jung, C.G., Watanabe, A., Lund-Katz, S., Pillips, M.C., Saito, H. and Michikawa, M., Mechanism underlying apolipoprotein E (ApoE) isoform-dependent lipid efflux from neural cells in culture, *J. Neurosci. Res.*, 87 (2009) 2498-2508.

[42] Mockel, B., zinke, H., Flach, R., Weis, B., Weiler-Guttler, H. and gassen, H.G., Expression of apolipoprotein A-I in porcine brain endothelium in vitro, *J. Neurochem.*, 62 (1994) 788-798.

[43] Mulder, M., Ravid, R., Swaab, D.F., De Kloet, E.R., Haasdijk, E.D., Julk, J., Van Der Boom, J.J. and Havekes, L.M., Reduced levels of cholesterol, phospholipids, and fatty acids in cerebrospinal fluid of Alzheimer disease patients are not related to apolipoprotein E4., *Alzheimer Dis. Assoc. Disord.*, 12 (1998) 198-203.

[44] Nagayasu, Y., Ito, J.-i., Nishida, T. and Yokoyama, S., Reactivity of astrocytes to fibroblast growth factor-1 for biogenesis of apolipoprotein E-high density lipoprotein is down-regulated by long-time secondary culture, *J. Biochem. (Tokyo)*, 143 (2008) 611-616.

[45] Nakagawa, T. and Schwartz, J.P., Expression of neurotrophic factors and cytokines and their receptors on astrocytes in vivo, *Advances in Molecular and Cell Biology*, 31 (2004) 561-573.

[46] Nishida, T., Ito, J.-i., Nagayasu, Y. and yokoyama, S., FGF-1-induced reactions for biogenesis of apoE-HDL are mediated by Src in rat astrocytes, *J. Biochem.*, 146 (2009) 881-886.

[47] Ornitz, D.M., J. Xu, J.S., Colvin, D.G., McEwen, C.A., MacArthur, F., Coulier, G. and Gao, M.G., Receptor apecificity of the fibroblast growth factor family, *J. Biol. Chem.*, 271 (1996) 15292-15297.

[48] Snipes, G.J., McGuire, C.B., Norden, J.J. and Freeman, J.A., Nerve injury stimulates the secretion of apolipoprotein E by nonneuronal cells, *Proc. Natl. Acad. Sci. U. S. A.*, 83 (1986) 1130-1134.

[49] Tada, T., Ito, J.-i., Asai, M. and yokoyama, S., Fibroblast growth factor 1 is produced prior to apolipoprotein E in the astrocytes after cryo-injury of mouse brain, *Neurochem. Int.*, 45 (2004) 23-30.

[50] Takami, K., Matsuo, A., Terai, K., Walker, D.G., McGeer, E.G. and McGeer, P.L., Fibroblast growth factor receptor-1 expression in the eoctex and hippocampus in Alzheimer's Disease, *Brain Res.*, 802 (1998) 89-97.

[51] Thorns, V. and Masliah, E., Evidense for neuroprotective efffects of acidic fibroblast growth factor in Alzheimer disease., *J. Neuropathol. Exp. Neurol.*, 58 (1999) 296-306.

[52] Tooyama, I., Akiyama, H., McGeer, P.L., hara, Y., yasuhara, O. and Kimura, H., Acidic fibroblast growth factor-like immunoreactivity in brain of Alzheimer patients, *Neurosci. Lett.*, 121 (1991) 155-158.

[53] Ueno, S., Ito, J.-i., Nagayasu, Y., Furukawa, T. and Yokoyama, S., An acidic fibroblast growth factor-like factor secretedinto the brain cell culture medium upregulates apoE synthesis, HDL secretion and cholesterol metabolism in rat astrocytes, *Biochim. Biophys. Acta*, 1589 (2002) 261-272.

[54] Wahrle, S.E., Jiang, H., Parsadanian, M., Hartman, R.E., Bales, K.R., Paul, S.M. and Holzman, D.M., Deletion of Abca1 increases Abeta deposition in the PDAPP transgenic mouse model of Alzheimer Disease, *J. Biol. Chem.*, 280 (2005) 43236-43242.

[55] Wahrle, S.E., Jiang, H., Parsadanian, M., Kim, J., Li, A., Knoten, A., Jain, S., Hirsch-Reinshagen, V., Wellington, C.L. and Bales, K.R., Overexpression of ABCA1 reduces amyloid deposition in the PDAPP mouse model of Alzheimer disease, *J. Clin. Invest.*, 118 (2008) 671-682.

[56] Wahrle, S.E., Jiang, H., Parsadanian, M., Legleiter, J., Han, X., Fryer, J.D., Kowalewski, T. and Holtzman, D.M., ABCA1 is required for normal central nervous system apoE levels and for lipidation of astrocytes-secreted apoE, *J. Biol. Chem.*, 279 (2004) 40987-40993.

[57] Wiedlocha, A., Nilsen, T., Wesche, J., Sorensen, V., Malecki, J., Marcinkowska, E. and Olsnes, S., Phosphorylation-regulated nucleocytoplasmic trafficking of internalized fibroblast growth factor-1, *Mol. Biol. Cell*, 16 (2005) 794-810.

[58] Zannis, V.I., McPherson, J., Goldberger, G., Karathanasis, S. and Breslow, j.L., Synthesis, intracellular processing, and signal peptide of human apolipoprotein E, *J. Biol. Chem.*, 259 (1984) 5495-5499.

[59] Zhao, Y. and Mazzone, T., Transport and processing of endogenously synthesized apoE on the macrophage cell surface, *J. Biol. Chem.*, 275 (2000) 4759-4765.

THE JOURNAL OF BIOLOGICAL CHEMISTRY VOL. 287, NO. 35, pp. 29362–29372, August 24, 2012

⌘ *Author's Choice*

Cell Surface Expression of the Major Amyloid-β Peptide (Aβ)-degrading Enzyme, Neprilysin, Depends on Phosphorylation by Mitogen-activated Protein Kinase/Extracellular Signal-regulated Kinase Kinase (MEK) and Dephosphorylation by Protein Phosphatase 1a*[S]

Received for publication, January 6, 2012, and in revised form, June 27, 2012 Published, JBC Papers in Press, July 5, 2012, DOI 10.1074/jbc.M112.340372

Naomasa Kakiya[‡§1], Takashi Saito[‡1], Per Nilsson[‡], Yukio Matsuba[‡], Satoshi Tsubuki[‡], Nobuyuki Takei[§], Hiroyuki Nawa[§], and Takaomi C. Saido[‡2]

From the [‡]Laboratory for Proteolytic Neuroscience, RIKEN Brain Science Institute, 2-1 Hirosawa, Wako-shi, Saitama 351-0198, Japan and the [§]Department of Molecular Neurobiology, Brain Research Institute, Niigata University, Niigata 951-8585, Japan

Background: Neprilysin is a major Aβ-degrading enzyme, the expression of which is reduced in the AD brain.
Results: The phosphorylation status of the neprilysin intracellular domain regulates localization and cell surface activity.
Conclusion: Regulation of neprilysin through phosphorylation influences Aβ levels.
Significance: Our results indicate that neprilysin phosphorylation/dephosporylation could be one druggable target in the development of an AD-modifying treatment.

Neprilysin is one of the major amyloid-β peptide (Aβ)-degrading enzymes, the expression of which declines in the brain during aging. The decrease in neprilysin leads to a metabolic Aβ imbalance, which can induce the amyloidosis underlying Alzheimer disease. Pharmacological activation of neprilysin during aging therefore represents a potential strategy to prevent the development of Alzheimer disease. However, the regulatory mechanisms mediating neprilysin activity in the brain remain unclear. To address this issue, we screened for pharmacological regulators of neprilysin activity and found that the neurotrophic factors brain-derived neurotrophic factor, nerve growth factor, and neurotrophins 3 and 4 reduce cell surface neprilysin activity. This decrease was mediated by MEK/ERK signaling, which enhanced phosphorylation at serine 6 in the neprilysin intracellular domain (S6-NEP-ICD). Increased phosphorylation of S6-NEP-ICD in primary neurons reduced the levels of cell surface neprilysin and led to a subsequent increase in extracellular Aβ levels. Furthermore, a specific inhibitor of protein phosphatase-1a, tautomycetin, induced extensive phosphorylation of the S6-NEP-ICD, resulting in reduced cell surface neprilysin activity. In contrast, activation of protein phosphatase-1a increased cell surface neprilysin activity and lowered Aβ levels. Taken together, these results indicate that the phosphorylation status of S6-NEP-ICD influences the localization of neprilysin and affects extracellular Aβ levels. Therefore, maintaining S6-NEP-ICD in a dephosphorylated state, either by inhibition of protein kinases involved in its phosphorylation or by activation of phosphatases catalyzing its dephosphorylation, may represent a new approach to prevent reduction of cell surface neprilysin activity during aging and to maintain physiological levels of Aβ in the brain.

Impaired metabolism of amyloid β peptide (Aβ)[3] in the brain is likely to play a central role in the pathogenesis of Alzheimer disease (AD) (1). Genetically, causative genes in familial AD link mutations in amyloid precursor protein (APP) and presenilins to aberrant increased generation of Aβ42 and Aβ43, the 42- and 43-mer forms of Aβ, respectively. Aβ42 and Aβ43 have higher amyloidogenecity and neural toxicity than Aβ40 (1–4) and lead to the early onset of AD. However, Aβ amyloidosis in sporadic AD, which comprises over 90% of all AD cases, may be caused by a decline in Aβ degradation, Aβ clearance, or both (5). We previously identified neprilysin as a major physiological Aβ-degrading enzyme that regulates the steady-state levels of Aβ species in the brain (6, 7). Consistent with the increase in Aβ levels observed during aging and in AD, the expression levels of neprilysin in the brain decrease with age and in the early stages of AD (8–12). Genetic ablation of neprilysin not only markedly accelerates amyloid plaque formation but also leads to increased impairment of synaptic plasticity and memory formation in APP transgenic mice (13, 14). In contrast, elevation of neprilysin expression/activity promotes Aβ degradation and reduces the accumulation of both soluble and fibrillary Aβ in APP transgenic mice (15–17). Based on these observations, we previously searched for factors that could increase neprilysin activity pharmacologically, identifying somatostatin as a nepri-

* This study was supported by research grants from RIKEN Brain Science Institute; the Ministry of Education, Culture, Sports, Science, and Technology; and the Ministry of Health, Labor, and Welfare of Japan. This study was also supported by the Junior Research Associate Program of RIKEN.
⌘ *Author's Choice*—Final version full access.
[S] This article contains supplemental Figs. S1–S6.
[1] Both authors contributed equally to this work.
[2] To whom correspondence should be addressed. Tel.: 81-48-467-9715; Fax: 81-48-467-9716; E-mail: saido@brain.riken.jp.

[3] The abbreviations used are: Aβ, amyloid β peptide; AD, Alzheimer disease; APP, amyloid precursor protein; BDNF, brain-derived neurotrophic factor; CTF, C-terminal fragment of APP; ICD, intracellular domain; NEP, neprilysin; hNEP, human NEP; NT, neurotrophin; PP1 and PP2, protein phosphatase-1 and -2, respectively; SFV, Semliki Forest virus; MCA, methyl cumaryl amide.

lysin up-regulator, although the underlining mechanisms remain unclear (18).

In this study, we investigated the effect of the neurotrophic factors brain-derived neurotrophic factor (BDNF), nerve growth factor (NGF), and neurotrophins 3 and 4 (NT-3 and -4) and found that they cause a reduction in cell surface neprilysin activity through MAPK signaling. Moreover, our results reveal that cell surface neprilysin activity and localization are regulated by phosphorylation and dephosphorylation at the neprilysin intracellular domain, with a reduction in neprilysin activity leading to an increase in Aβ levels. We therefore speculate that possible drug targets involving neprilysin could include factors involved in the phosphorylation/dephosphorylation of this Aβ-lowering enzyme.

EXPERIMENTAL PROCEDURES

Materials—The reagents used in this study were purchased as follows: BDNF, NGF, NT-3, NT-4, cyclosporin A, and FK-506 (Sigma); U0126 (Enzo Life Sciences); fostriecin, okadic acid, and tautomycetin (Calbiochem); and recombinant human neprilysin (R&D Systems). The phospho-human neprilysin antibodies pS4-NEP, pS6-NEP, pT11-NEP, pT15-NEP, and pT25-NEP were obtained by immunizing rabbits with the following respective synthetic peptides containing phosphoserine (pS) or phosphothreonine (pT) residues: GKpSESQMC, GKSEpSQC, QMDIpTDINTC, TDINpTPKPKC, and KQRWpTPLEC (19, 20). The specificities of the purified phosphoantibodies were investigated by dot blot analysis (21) (see supplemental Fig. S3).

Cell Culture—Human SH-SY5Y neuroblastoma cells were obtained from the European Collection of Cell Cultures. Cells were cultured in 5% CO_2 at 37 °C, as previously described (22). The medium comprised a 1:1 mixture of minimum essential medium and Ham's F-12 medium (Nacalai Tesque), supplemented with 1 μM non-essential amino acids, 100 units/ml penicillin, 100 mg/ml streptomycin, and 15% fetal bovine serum (Invitrogen). Primary cortical/hippocampal neurons derived from wild-type or neprilysin-deficient mouse embryos were isolated as described previously (18). The neurons were plated at 5.0×10^4 cells/well in 96-well plates, 2.0×10^5 cells on glass coverslips (Hamanami) placed in 24-well plates, or 1.0×10^6 cells/well in 6-well plates. After 14 days *in vitro*, primary neurons were subjected to the various assays.

Mutagenesis and Transfection—S4A-, S6A-, T11A-, T15A- and T25A-human neprilysin mutants were generated using a KOD-Plus mutagenesis kit (Toyobo) according to the manufacturer's protocol. To introduce the mutations into human neprilysin cDNA previously cloned into pcDNA3.1 (23), the following primer sets were designed: S4A, 5′-GCAGAAAGTCAGATGGATATA-3′ and 5′-CTTGCCCATCACCTAGGCTGC-3′; S6A, 5′-GCTCAGATGGATATAACTGATATC-3′ and 5′-TTCTGACTTGCCCATCACCTAGG-3′; T11A, 5′-GCTGATATCAACACTCCAAAGC-3′ and 5′-TATATCCATCTGACTTTCTG-3′; T15A, 5′-GCTCCAAAGCCAAAGAAGAAACAGC-3′ and 5′-GTTGATATCAGTTATATCCATCTG-3′; and T25A, 5′-GGCTCCACTGGAGATCAGCCTCTCG-3′ and 5′-CATCGCTGTTTCTTCTTTGGCTTTG-3′ (underlined, original T, AG, A, A, and A, respectively). Constitutive active protein phosphatase-1a (PP1a)-T320A (24) was generated using the KOD-Plus mutagenesis kit, using the following primer set: 5′-GCCCCACCCCGCAATTCCGCCAAA-3′ and 5′-GATGGGTCGGCCTCCAGGGTTCAG-3′ (underlined, original A to G mutation). The mutant genes were transfected into SH-SY5Y cells using FuGENE transfection reagent (Roche Applied Science) according to the manufacturer's instructions. Cells were harvested with lysis buffer containing 0.1 M Tris-HCl, pH 7.5, EDTA-free complete protease inhibitor mixture (Roche Applied Science), 1% Triton X-100, 0.15 M NaCl, 1 mM Na_3VO_4, 1 mM NaF, and 1 μg/ml pepstatin A (Peptide Institute) 48–72 h after transfection.

Cell Surface and Whole-cell Neprilysin Activity—Activity staining of neprilysin using primary neurons was performed as described previously (18), with slight modifications. Because the endogenous neprilysin activity was too low in the primary neurons and SH-SY5Y cells, the cells were infected with Semliki Forest virus containing human neprilysin cDNA (SFV-hNEP), as previously described (25). Twenty-four h postinfection at day *in vitro* 14, neurotrophic factors or other reagents were added, and the cells were incubated for 24 h. They were then fixed with 1.5% paraformaldehyde in 50 mM phosphate buffer (pH 6.8) for 5 min at room temperature. The fixed neurons were incubated in substrate solution (0.25 mM glutaryl-Ala-Ala-Phe-methoxy-2-naphthylamide in 50 mM Tris-HCl, pH 7.4) at 37 °C for 2 h. Leucine aminopeptidase (Sigma), phosphoramidon (Peptide Institute), and nitrosalicylaldehyde (Sigma-Aldrich) were then added to the substrate solution at a final concentration of 50 μg/mg, 10 μM, and 0.6 mM, respectively, and incubated for 30 min at 37 °C. Quantification of the fluorescence signal arising from cell surface neprilysin activity was performed as described previously (18). Cell surface and whole-cell neprilysin activity of SH-SY5Y cells expressing mutant neprilysin were measured as described previously (26), with slight modifications (supplemental Fig. S5). Before the addition of neurotrophic factors, the cells were starved for 48 h to eliminate the effect of serum. After a 24-h treatment with neurotrophic factors, cells or lysates were incubated with substrate mixture (50 μM suc-Ala-Ala-Phe-MCA (Peptide Institute) and 10 nM benzyloxycarbonyl (Z)-Leu-Leu-Leucinal in 50 mM MES, pH 6.5, with or without 10 μM thiorphan (neprilysin-specific inhibitor)) at 37 °C for 30 min. Following this, 0.1 mg/ml leucine aminopeptidase (Sigma) and 0.1 mM phosphoramidon were added, and the reaction mixture was incubated at 37 °C for a further 30 min. 7-Amino-4-methylcoumarin fluorescence was measured at excitation and emission wavelengths of 380 and 460 nm, respectively. After measurement, cells were collected and subjected to Western blot analysis to evaluate neprilysin levels.

Cell Surface Biotinylation—The cell membrane of cortical/hippocampal neurons or SH-SY5Y cells was biotinylated with sulfo-NHS-SS-biotin (Pierce), according to the manufacturer's instructions. The samples were subsequently subjected to immunocytochemical study or pull-down assay. Biotinylated cell surface proteins were pulled down using Biotin-Capture beads (Adar Biotech).

Immunocytochemical Study—To visualize and quantify neprilysin localization in cortical/hippocampal neurons, the cells were infected with SFV-hNEP, and the cell surface was

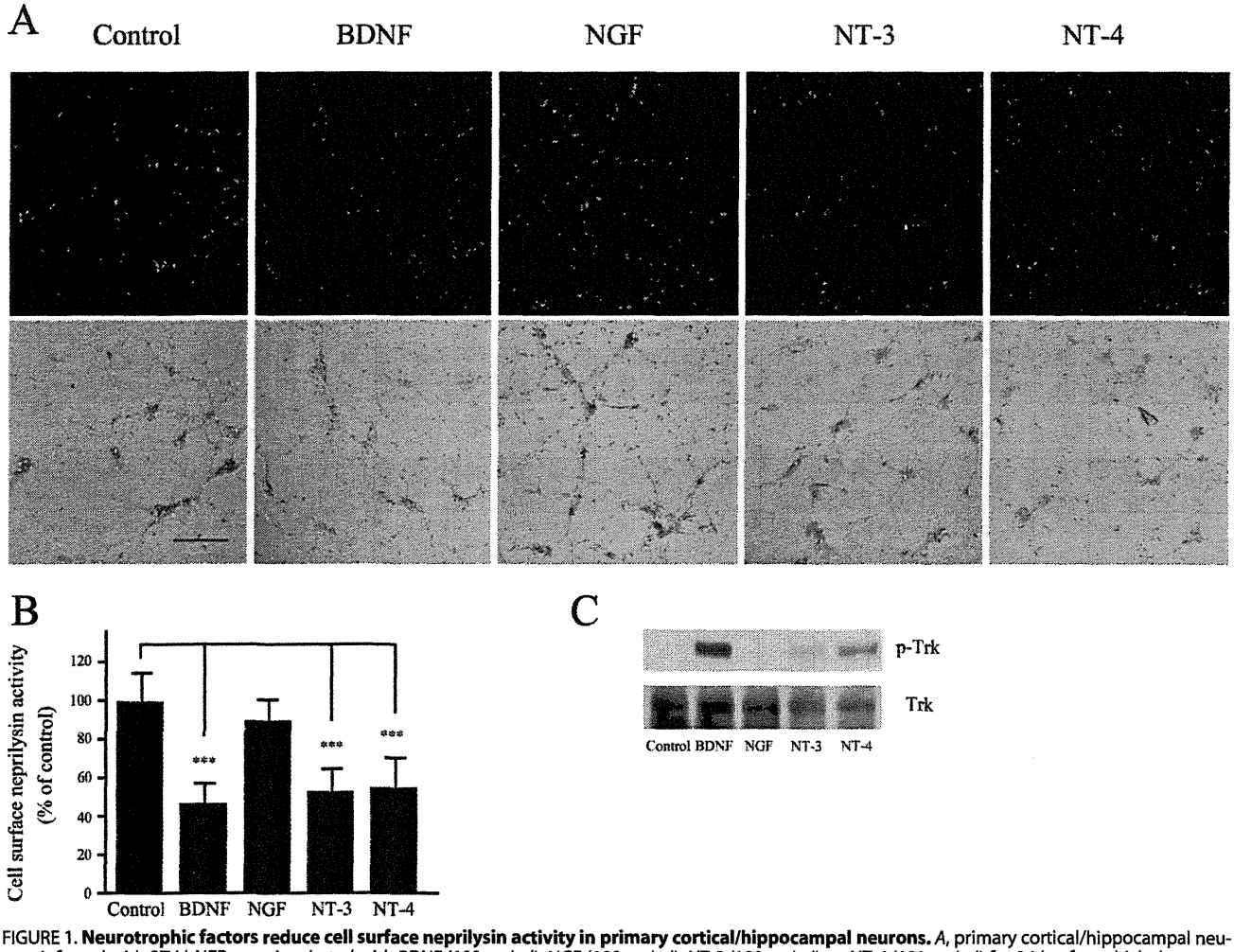

FIGURE 1. **Neurotrophic factors reduce cell surface neprilysin activity in primary cortical/hippocampal neurons.** *A*, primary cortical/hippocampal neurons infected with SFV-hNEP were incubated with BDNF (100 ng/ml), NGF (100 ng/ml), NT-3 (100 ng/ml), or NT-4 (100 ng/ml) for 24 h, after which they were subjected to the neprilysin activity-staining assay. The *top panels* show fluorescence images representing neprilysin activity, and the *bottom panels* show phase-contrast images merged with the *top panels*. *Scale bar*, 100 μm. *B*, quantification of the fluorescence signal areas, indicated as average ± S.D. (*error bars*) ($n = 5$). ***, $p < 0.01$ compared with control. *C*, primary neurons were incubated with BDNF (100 ng/ml), NGF (100 ng/ml), NT-3 (100 ng/ml), or NT-4 (100 ng/ml) for 30 min and then subjected to Western blot analysis to measure the phosphorylation level of the neurotrophic factor receptor, Trk, using antibodies against Trk receptor (*bottom*) and phosphorylated Trk (*p-Trk; top*). At least three independent experiments were repeated.

labeled with biotin. The cells grown on coverslips were fixed with 100% ice-cold MeOH for 10 min at −20 °C and permeabilized in 100% ice-cold acetone for 1 min at −20 °C. After blocking with blocking buffer (phosphate-buffered saline containing 5% skim milk, 5% goat serum, and 0.05% Tween 20) for 30 min at room temperature, the samples were incubated with primary anti-human neprilysin antibody (1:100, Novocastra) in blocking buffer for 1 h at room temperature, followed by secondary anti-mouse Alexa 488 (1:500, Invitrogen) and Streptavidin-Alexa 546 (1:500; Molecular Probes) antibody for 30 min at room temperature. The fluorescence signals observed by confocal microscopy were quantified by counting signal dots, as described previously (27).

Immunoprecipitation and Western Blot Analysis—Cell lysates from primary cortical/hippocampal neurons infected with SFV-hNEP were immunoprecipitated with mouse monoclonal anti-human neprilysin (SN5c/L4–1A1, Ancell). Samples were subjected to Western blot analysis using the following antibodies: phospho-human neprilysin antibodies (supplemental Fig. S3), anti-human neprilysin (56C6, Novocastra), anti-mouse neprilysin (421126, Techne), antibodies recognizing the N-terminal region of APP (22C11, Chemicon) or the C-terminal region of APP (A8717, Sigma), anti-PP1A (Thr(P)-320) (EP1512Y, Novus), anti-PP1α (Santa Cruz Biotechnology, Inc., Santa Cruz, CA), anti-phospho-TrkA (Tyr-490, Cell Signaling), anti-Trk (B-3, Cell Signaling), anti-phospho-Erk1/2 (Thr-202/Tyr-204, Cell Signaling), anti-Erk1/2 (Cell Signaling), anti-Myc (9B11, Cell Signaling), anti-G3PDH/GAPDH (Trevigen), or anti-β-actin (AC-15, Sigma-Aldrich).

Aβ ELISA—Conditioned medium from control cortical/hippocampal neurons or those treated with neurotrophic factors for 24 h and from SH-SY5Y cells transiently expressing wild-type neprilysin (WT-NEP), S6A-NEP, WT-PP1a, and T320A-PP1a were collected, and guanidine HCl was added as described previously (4). In order to achieve a measurable level of Aβ40 in the conditioned medium from SH-SY5Y cells transfected with WT-NEP or S6A-NEP, 200 pM Aβ40 peptide was added to the samples. Samples were analyzed using Aβ-ELISA kits (Wako)

to quantify Aβ40 and Aβ42, according to the manufacturer's instructions.

Statistical Analysis—All of the values are presented as mean ± S.D. Statistical analysis was performed by one-way analysis of variance with Scheffe's F test.

RESULTS

Neurotrophic Factors Reduce Neprilysin Activity via MAPK Signal Transduction—Membrane-bound neprilysin located on the cell surface participates in extracellular Aβ degradation and therefore plays a key role in Aβ metabolism. We have previously established an activity-staining method for primary neurons that visualizes neprilysin activity on the cell surface (18, 25). In a search for regulators of neprilysin activity, we identified somatostatin, which was found to exert an up-regulatory effect (18). To further unravel the mechanisms regulating neprilysin activity, we screened the neurotrophic factors BDNF, NGF, NT-3, and NT-4 using our activity-staining technique on primary cortical/hippocampal neurons. Representative images of such activity-staining experiments are shown in Fig. 1. Interestingly, BDNF, NT-3, and NT-4 all significantly reduced neprilysin activity, whereas NGF had no effect. However, given that cortical/hippocampal neurons do not express the TrkA receptor subtype to which NGF binds (28), we also examined the effect of NGF on primary neurons derived from the striatum. Indeed, exposing striatal primary neurons to NGF induced a reduction in neprilysin activity (supplemental Fig. S1, *A* and *B*). To confirm activation of the signal transduction pathway leading to a reduction in neprilysin, phosphorylation of Tyr-490 in Trk was measured (29). Upon exposure of the primary neurons to BDNF, NGF, NT-3, or NT-4, phosphorylation of Trk significantly increased (Fig. 1*C* and supplemental Fig. S1*C*), indicating that the Trk receptors were activated.

To further elucidate the Trk receptor-induced transduction pathway, we next investigated the effects of U0126, LY294002, and calphostin C, inhibitors of MAPK/ERK kinase 1/2 (MEK1/2), phosphatidylinositol-3 kinase, and protein kinase C, respectively, on cell surface neprilysin activity (30). First, we co-treated neurons with BDNF, NGF, NT-3, or NT-4 together with U0126 and found that U0126 completely inhibited the reduction in cell surface neprilysin activity induced by the neurotrophic factors (Fig. 2), indicating the involvement of MAPK/ERK kinase in the signaling pathway. We then focused on NT-3 because it binds to all Trk receptor subtypes (*i.e.* TrkA, -B, and -C) (28). Simultaneous treatment of neurons with NT-3 and calphostin C did not inhibit the reduction in neprilysin activity. Finally, LY294002 treatment alone produced a decrease in cell surface neprilysin activity. However, because LY294002 in combination with NT-3 did not inhibit the NT-3-induced reduction in neprilysin activity (supplemental Fig. S1*D*), it is possible that the effect of LY294002 involves a pathway independent of the Trk signaling pathway. Thus, together these results indicate that neurotrophic factors reduce cell surface neprilysin activity in neurons via the MEK/ERK signaling pathway.

Although binding of neurotrophic factors to Trk receptors is known to activate the MAPK pathway within 30 min (31) (Fig. 1*C*), the levels of cell surface neprilysin activity remained unaltered 30 min after the addition of the neurotrophic factors (supplemental Fig. S1*E*). Rather, the effect became clearly visible 24 h poststimulation (Fig. 1, *A* and *B*). Taken together, these findings indicate that neurotrophic factors reduce cell surface neprilysin activity by binding to neuronal Trk receptors and subsequent activation of the MAPK pathway. The mechanistic explanation behind the delayed effect is currently not known but could include changes in, for example, gene expression of additionally required factors.

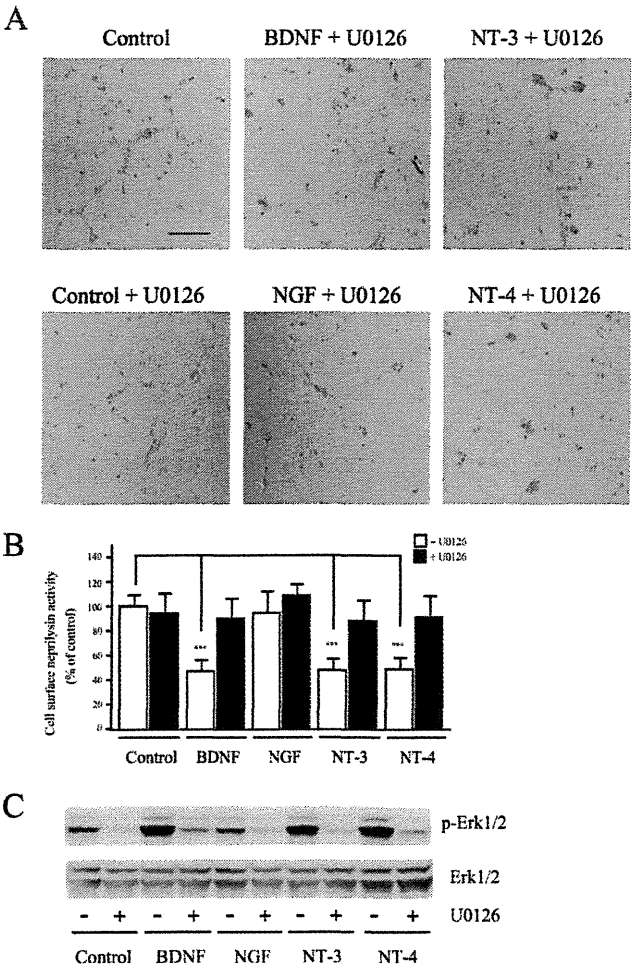

FIGURE 2. **Reduction of neprilysin activity by neurotrophic factors involves the MEK1/2 signaling pathway.** *A*, primary cortical/hippocampal neurons infected with SFV-hNEP were co-incubated with BDNF (100 ng/ml), NGF (100 ng/ml), NT-3 (100 ng/ml), or NT-4 (100 ng/ml) and the MEK1/2 inhibitor U0126 (1 μM), for 24 h, after which they were subjected to the neprilysin activity-staining assay. Representative fluorescence images merged with phase-contrast images are shown. *Scale bar*, 100 μm. *B*, quantification of the fluorescence signal derived from neprilysin activity was performed, and the results are presented as average ± S.D. (*error bars*) ($n = 5$). ***, $p < 0.01$ compared with control. *C*, primary neurons were incubated with or without U0126, as indicated, and neurotrophic factors for 30 min and were then subjected to Western blot analysis to measure the phosphorylation levels of MAPK using antibodies against Erk1/2 (*bottom*) and phosphorylated Erk1/2 (*p-Erk1/2; top*). At least three independent experiments were repeated.

Effect of NT-3 on Aβ Levels—A reduction in neprilysin induced by neurotrophic factors would presumably lead to increased Aβ levels. We therefore measured Aβ levels in conditioned medium from primary neurons infected with SFV-hNEP, using the same conditions as for the activity assay. How-

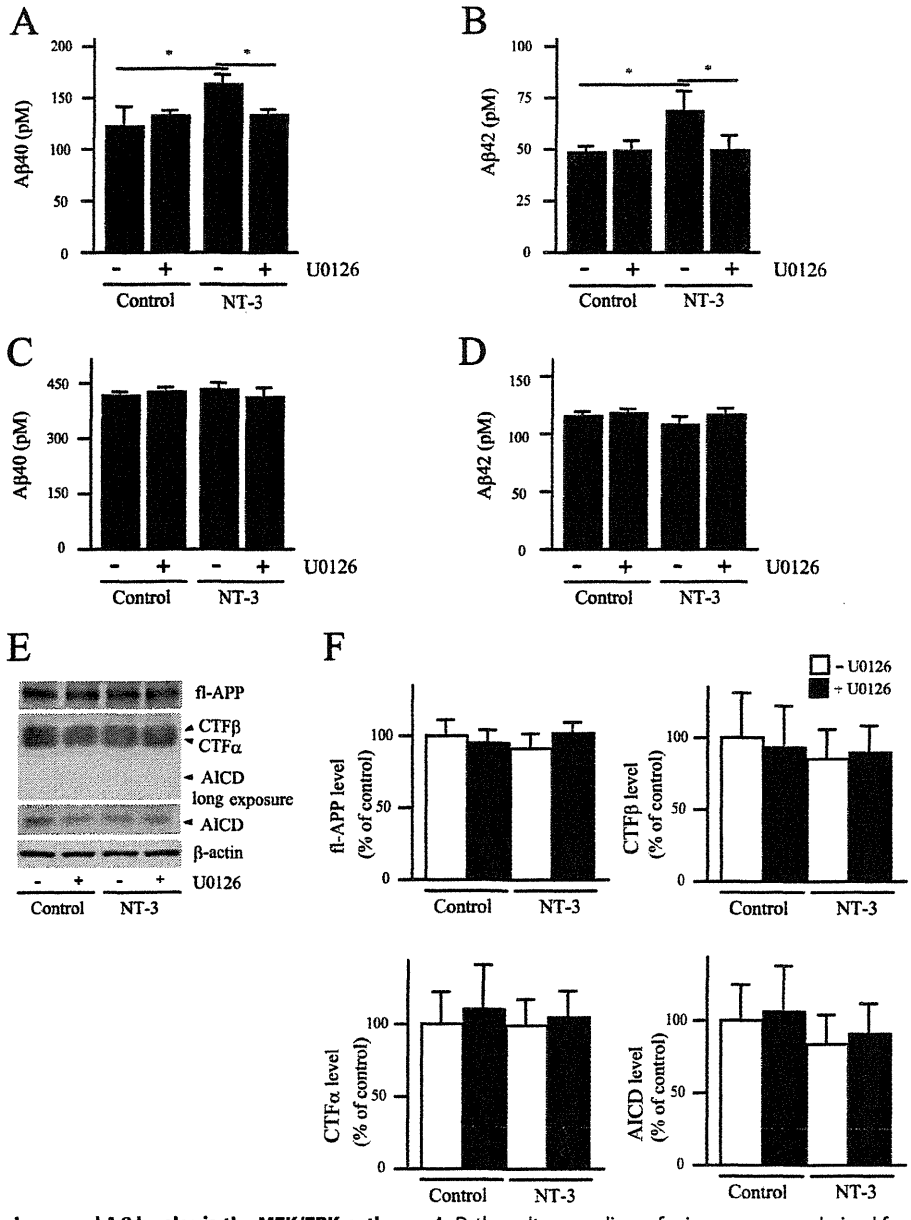

FIGURE 3. **NT-3 induces increased Aβ levels via the MEK/ERK pathway.** *A–D*, the culture medium of primary neurons derived from wild-type (*A* and *B*) or NEP-deficient mouse embryos (*C* and *D*) was collected 24 h after NT-3 (100 ng/ml) treatment with or without U0126 (1 μM) and then subjected to Aβ ELISA. Aβ40 (*A* and *C*) and Aβ42 (*B* and *D*) levels were measured using an Aβ-ELISA kit. Each *column* with *error bar* represents the mean ± S.D. ($n = 4$). *, $p < 0.05$ compared with control and co-treatment. *E* and *F*, the effect of neurotrophic factors on Aβ generation was investigated by measuring the levels of full-length APP (*fl-APP*), CTFα, CTFβ, APP intracellular domain (*AICD*), and β-actin in the primary neurons by Western blot. Intensities of each band were quantified by densitometric analysis, and data represent the mean ± S.D. ($n = 5$).

ever, due to the high viral expression of neprilysin, the Aβ levels were too low to be detected. Therefore, we instead measured the conditioned medium from non-infected primary cortical/hippocampal neurons. NT-3 treatment significantly increased the steady-state levels of Aβ40 and Aβ42, an effect that was abolished by the addition of U0126 (Fig. 3, *A* and *B*). Importantly, treating primary neurons derived from neprilysin-deficient mice with NT-3 did not affect Aβ levels, showing that the increased Aβ levels generated from wild-type neurons are due specifically to a decrease in neprilysin activity (Fig. 3, *C* and *D*). Furthermore, full-length APP levels and the levels of the C-terminal fragments of APP, CTFα, CTFβ, and APP intracellular domain, which are produced by α-, β- and γ-secretase, respectively, and used as an index of secretase activity (32) were not altered by NT-3 treatment (Fig. 3, *E* and *F*). These results together suggest that the increased steady-state levels of Aβ upon NT-3 treatment are due specifically to a decrease in cell surface neprilysin activity rather than increased Aβ generation in the neurons. Finally, to ascertain that the increased Aβ levels observed upon NT-3 treatment were specifically due to decreased levels of cell surface neprilysin, the levels of the Aβ-degrading enzymes endothelin-converting enzyme-1 (33) and insulin-degrading enzyme (34) were investigated. Neither the levels of endothelin-converting enzyme-1 and insulin-

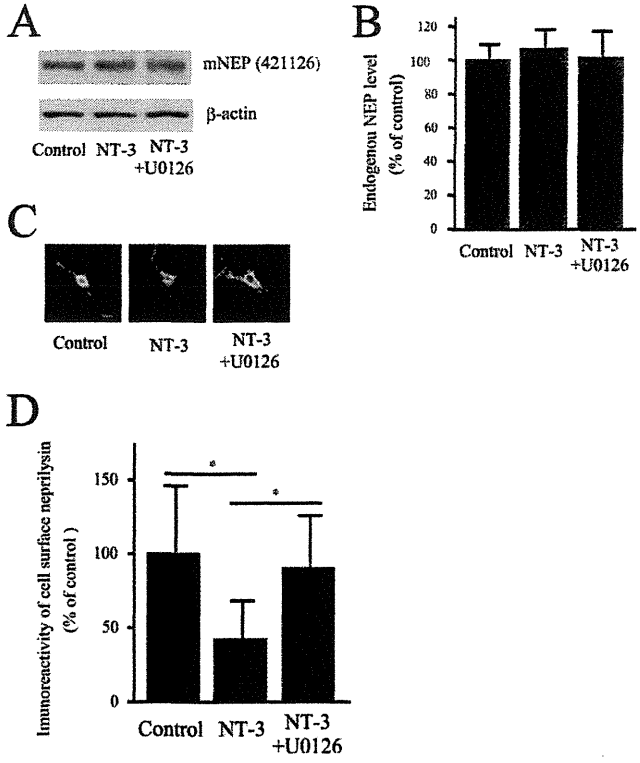

FIGURE 4. **NT-3 regulates neprilysin localization via the MEK/ERK pathway.** *A* and *B*, the effect of NT-3 on expression levels of neprilysin in primary neurons was analyzed by Western blot analysis. The experiments were repeated four times, and the results are presented as mean values ± S.D. (*error bars*). *C* and *D*, double staining for neprilysin and biotinylated proteins located on the cell surface. Primary cortical neurons infected with SFV-hNEP were treated with NT-3 (100 ng/ml) for 24 h. The cell surface proteins were subsequently cross-linked with biotin, after which the cells were double-stained with neprilysin antibody (56C6; *green*) and Alexa 546-conjugated streptavidin (*red*). The images of the *green* and the *red* signals were merged, *yellow* representing cell surface neprilysin. *Scale bar*, 50 μm. The ratio of cell surface neprilysin levels was quantified by image analysis. Data represent the mean ± S.D. ($n = 15$). *, $p < 0.05$ compared with control and co-treatment.

degrading enzyme nor the activity of insulin-degrading enzyme were affected by NT-3 treatment (supplemental Fig. S2, *A* and *B*). These data, together with the lack of changes in Aβ levels secreted from primary neurons prepared from neprilysin knock-out mice and stimulated with neurotrophic factors, lead us to conclude that decreased levels in cell surface neprilysin expression are responsible for the increased Aβ levels.

NT-3 Alters Neprilysin Localization in Neurons—To address whether the NT-3-induced reduction in neprilysin was due to changes in neprilysin expression, we quantified neprilysin levels in whole-cell lysates before and after NT-3 treatment. Western blot data clearly showed that neprilysin expression levels were not altered after NT-3 treatment (Fig. 4, *A* and *B*). Therefore, we next performed immunocytochemical experiments to visualize neprilysin in the neurons. Proteins located on the cell surface were biotinylated, after which the cells were immunocytochemically stained with avidin and anti-neprilysin antibody and analyzed as described under "Experimental Procedures." Quantitative image analysis revealed that the level of neprilysin located on the cell surface was significantly reduced upon NT-3 treatment (Fig. 4, *C* and *D*). Importantly, the addition of U0126 restored this level to normal. Taken together, these results indicate that neurotrophic factors modulate neprilysin localization through MEK/ERK signaling, without affecting neprilysin expression levels, leading to a decrease in cell surface neprilysin activity and ultimately resulting in increased extracellular Aβ levels.

MEK/ERK Signaling Modulates the Phosphorylation State of the Neprilysin Intracellular Domain—The localization of plasma membrane-associated proteins is often regulated by phosphorylation/dephosphorylation at the intracellular domain (ICD) of the protein (35). Because neprilysin is a type II membrane protein, its N-terminal side is located in the cytoplasmic lumen. As shown in Fig. 5*A*, there are five potential amino acid residues in human neprilysin and four in mouse neprilysin ICD (NEP-ICD) that could possibly be phosphorylated. In order to accurately determine the phosphorylation state of the NEP-ICD, we first generated the phosphoserine- and phosphothreonine-specific antibodies pS4-NEP, pS6-NEP, pT11-NEP, pT15-NEP, and pT25-NEP, which specifically recognize individual phosphorylated threonine and serine residues in the NEP-ICD, respectively. The specificities of these antibodies are summarized in supplemental Fig. S3. We then probed cell extracts of primary neurons using this battery of phospho-antibodies. Although the endogenous expression level of neprilysin is low, we were able to detect phosphorylation of Ser-4, Ser-6, and Thr-11 in neprilysin (Fig. 5). We were not able to detect pT25-NEP due to limited affinity of the antibody. Interestingly, upon exposing primary neurons to NT-3, phosphorylation of Ser-6 increases significantly. Simultaneously treating the cells with NT-3 and U0126 inhibited the increase in phosphorylation of Ser-6 induced by NT-3, implying that the MAPK pathway is involved in the regulation of NEP-ICD phosphorylation (Fig. 5, *B* and *C*).

Because the endogenous neprilysin level in primary neurons is low and our aim was to study the regulatory mechanism of human neprilysin, we continued our studies using SFV-hNEP-infected primary neurons. After infection, we investigated the phosphorylation state of NEP-ICD. Consistent with phosphorylation of Ser-6 of endogenous neprilysin, we detected that overexpressed human neprilysin also was phosphorylated at Ser-6 upon treatment with NT-3. Further, the effect was inhibited by the addition of U0126. In addition, a trend toward increased Ser-4 phosphorylation was detected together with increased phosphorylation of Thr-15 (Fig. 5, *B* and *C*). Subsequently, we examined whether neprilysin localized to the cell surface exhibits different phosphorylation statuses compared with intracellularly located neprilysin. Biotinylated proteins located on the cell surface of SFV-hNEP-infected primary neurons were first pulled down from cell lysates using Biotin-Capture beads, after which intracellular neprilysin was collected using a neprilysin-specific antibody. Although all potential phosphorylation sites in the NEP-ICD of intracellularly located neprilysin were phosphorylated, no phosphorylation of Ser-6 or Thr-25 could be detected in neprilysin present in the cell surface fraction (Fig. 5*D*). These results together indicated that treating the cells with NT-3 for 24 h resulted in extensive phosphorylation of Ser-6 and Thr-15 of cell surface-located neprilysin. Although activation of Trk receptors was detected 30 min

after the addition of NT-3 to the cells, there was no difference in the phosphorylation state of NEP-ICD after a 30-min treatment by NT-3 (data not shown). The reasons behind the delayed effect are currently not known. Furthermore, the increase in phosphorylation of Ser-4, Ser-6, and Thr-15 induced by NT-3 was inhibited by the addition of U0126, indicating the involvement of MAPK in the signaling pathway (Fig. 5, *B* and *C*). Together, the data indicate that phosphorylation of Ser-6 is involved in the regulation of cell surface neprilysin.

To further clarify the role of human NEP-ICD phosphorylation in neprilysin activity, we generated five mutants in which

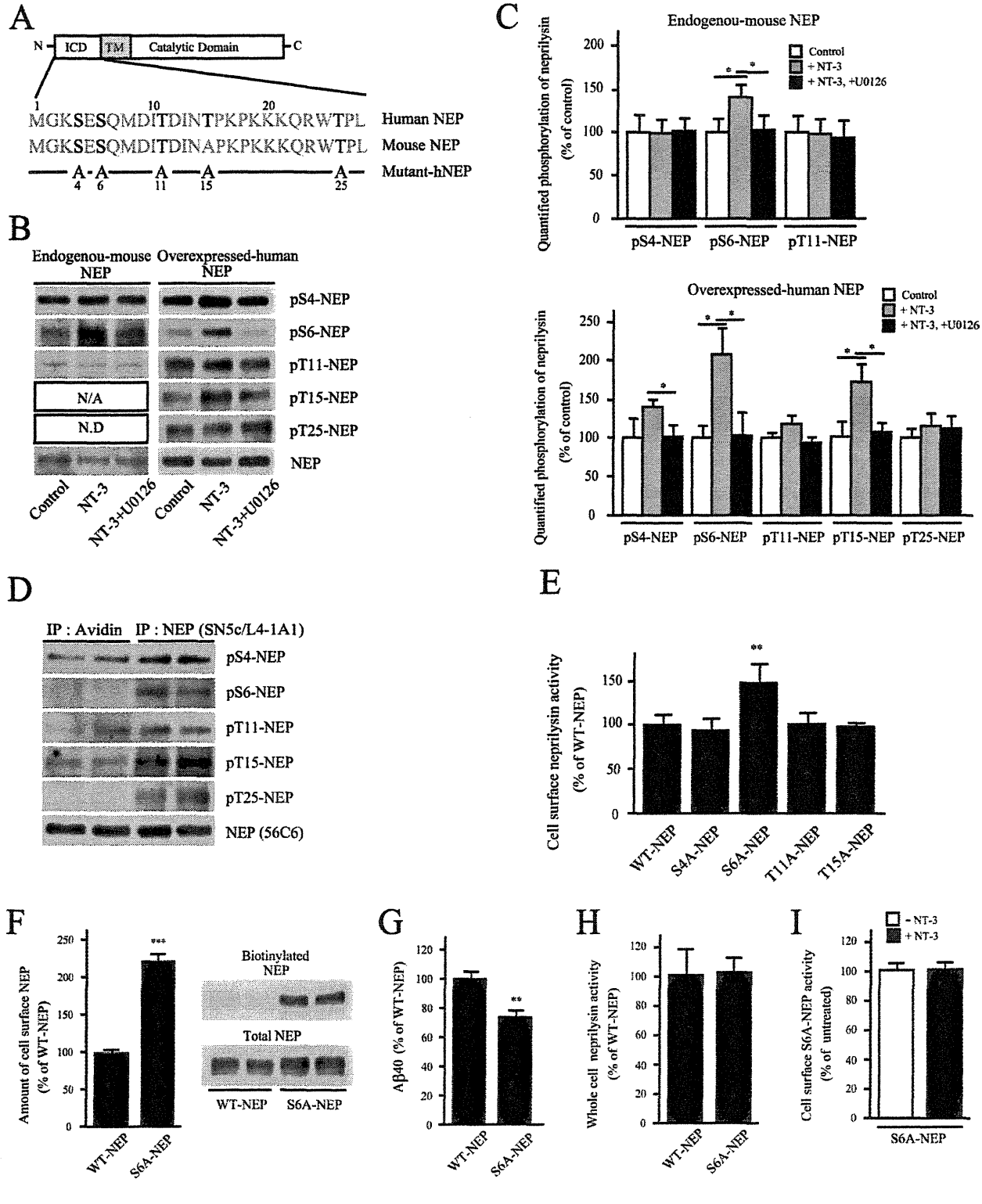

the putative serines/threonines in the NEP-ICD were substituted with alanines (*i.e.* S4A-, S6A-, T11A-, T15A-, and T25A-NEP, respectively) (Fig. 5*A*). The selection of a cell line for the mutational analysis was based on two criteria: 1) it should be a human neuronal cell line, and 2) it should express endogenous neprilysin to assure that the regulatory mechanisms of neprilysin are preserved. The endogenous expression of neprilysin in SH-SY5Y was confirmed with Western blot (Fig. S5*A*). Thus, the mutants were introduced into SH-SY5Y cells, and cell surface neprilysin activity was measured and normalized to expression levels. Interestingly, S6A-NEP transfectants showed significantly higher cell surface activity than S4A-, T11A-, T15A-, and WT-NEP transfectants (Fig. 5*E* and supplemental Fig. S4). The effect of T25A-NEP on neprilysin activity could not be evaluated due to its low expression (supplemental Fig. S5). We also subsequently measured the amount of cell surface-located S6A-NEP and found it to be significantly higher than that of WT-NEP (Fig. 5*F*). In accordance with the increased cell surface activity of S6A-NEP, the extracellular Aβ40 level in conditioned medium from S6A-NEP transfectants was significantly lower than that for WT-NEP transfectants (Fig. 5*G*). Furthermore, the total neprilysin activity, normalized to expression levels, in whole-cell lysates from WT-NEP and S6A-NEP transfectants were similar (Fig. 5*H*). This indicates that the increase in cell surface neprilysin activity observed in the case of S6A-NEP was not due to an allosteric effect induced by the mutation. Last, the cell surface neprilysin activity of S6A-NEP transfectants was not affected by NT-3 treatment (Fig. 5*I*). Taking all of the data together, we conclude that phosphorylation of Ser-6 of the NEP-ICD regulates neprilysin localization and thereby neprilysin cell surface activity via MEK/ERK signaling.

PP1a Facilitates Cell Surface Neprilysin Activity—Given that phosphorylation of Ser-6 in the NEP-ICD influences neprilysin cell surface localization, we next evaluated the effects of different phosphatase activities on neprilysin localization and activity. Primary cortical/hippocampal neurons infected with SFV-hNEP were treated with the following specific inhibitors for serine/threonine phosphatases: tautomycetin (PP1a inhibitor), fostriecin and okadaic acid (PP2A inhibitors), and cyclosporin A and FK-506 (PP2B/calcineurin inhibitors). Interestingly, treatment with the PP1a inhibitor tautomycetin resulted in significantly increased phosphorylation of the S6-NEP-ICD (Fig. 6, *A* and *B*) and decreased cell surface neprilysin activity (Fig. 6*C*). In addition to S6-NEP-ICD, phosphorylation of S4- and T11-NEP-ICDs was also increased by tautomycetin. However, phosphorylation of Ser-4 and Thr-11 did not influence cell surface neprilysin activity (Fig. 5 and supplemental Fig. S6).

The increased phosphorylation of Ser-6 upon PP1a inhibition suggests an association of neprilysin and PP1a. Previously, PTEN (phosphatase and tensin homolog deleted from chromosome 10), which is a tumor suppressor and acts as a tyrosine phosphatase, has been shown to be associated with the NEP-ICD (36). Interestingly, an amino acid sequence found in the NEP-ICD, KKKQRW, is similar to a PP1a-interacting sequence (37, 38). This finding prompted us to investigate a possible interaction between neprilysin and PP1a. We therefore performed immunoprecipitation experiments using SH-SY5Y cell lysates from mock and WT-NEP transfectants. The results revealed that neprilysin co-immunoprecipitates not only with PTEN but also with PP1a, indicating that the proteins are directly or indirectly associated (Fig. 6*D*).

To confirm the role of PP1a in neprilysin dephosphorylation and localization, and because PP1a is activated by dephosphorylation at the threonine 320 residue, we prepared a constitutive active mutant PP1a, which harbors a T320A mutation (Fig. 6*E*) (24). Expression of both WT-PP1a and T320A-PP1a in SFV-hNEP-infected SH-SY5Y cells induced an increase in cell surface neprilysin activity compared with mock transfectants. Moreover, constitutive active T320A-PP1a transfectants exhibited significantly higher cell surface neprilysin activity compared with WT-PP1a transfectants (Fig. 6*F*).

In addition, extracellular Aβ levels were significantly reduced by both WT-PP1a and T320A-PP1a expression (Fig. 6*G*). Taken together, these results suggest that activation of PP1a increases cell surface neprilysin activity/localization is due, at least partly, to dephosphorylation of Ser-6 in the NEP-ICD.

DISCUSSION

Pharmacological maintenance or enhancement of the major Aβ-degrading enzyme neprilysin during aging could offer a possible treatment for the prevention of AD. Accumulating evi-

FIGURE 5. **Dephosphorylation of the neprilysin intracellular domain localizes neprilysin to the cell surface.** *A*, scheme of human and mouse neprilysin domain structure and the N-terminal amino acid sequences corresponding to the neprilysin intracellular domain. *ICD* and *TM*, intracellular domain and transmembrane domain of neprilysin, respectively. Potential phosphorylation sites are indicated in *boldface type*. *Below*, the substituted serines/threonines to alanines are indicated in the five phosphoneprilysin mutants, S4A-, S6A-, T11A-, T15A-, and T25A-NEP. *B*, effects of NT-3 on the phosphorylation state of the intracellular domain of neprilysin. Primary neurons (*left*) were untreated or treated with NT-3 (100 ng/ml) or NT-3 together with U0126 for 24 h, as indicated, after which neprilysin was immunoprecipitated from 1 mg of cell lysate with neprilysin antibody, and the immunoprecipitates were analyzed by immunoblotting with phosphoneprilysin antibodies. Primary neurons expressing human neprilysin by infection with SFV-hNEP (*right*) were treated the same way as the non-infected primary neurons, as indicated. 150 μg of cell lysate was immunoprecipitated and immunoblotted with phosphoneprilysin antibodies, as indicated to the *right*. *N/A*, not applicable; *N.D*, not determined. *C*, densitometric quantification of Western blot data in *B*. Data represent the mean ± S.D. (*error bars*) ($n = 3$). *, $p < 0.05$, treated sample compared with non-treated or co-treated. *D*, cell surface-located proteins were biotinylated and pulled down using streptavidin beads, followed by immunoprecipitation (*IP*) of non-biotinylated neprilysin using a neprilysin antibody. Immunoprecipitates were subjected to Western blot analysis using the phosphoneprilysin antibodies pS4-NEP, pS6-NEP, pT11-NEP, pT15-NEP, pT25-NEP, and NEP (56C6). Western blot data of samples from two independent experiments are shown. At least three independent experiments were performed, and a similar band pattern was repeatedly verified. *E*, cell surface neprilysin activity of SH-SY5Y cells transiently expressing WT-, S4A-, S6A-, T11A-, T15A-, or T25A-NEP were evaluated using suc-Ala-Ala-Phe-MCA substrate. The neprilysin activities were normalized to neprilysin expression levels quantified by Western blot. Data represent the mean ± S.D. ($n = 3$). **, $p < 0.01$ compared with WT-NEP. *F*, SH-SY5Y cells transiently expressing WT-NEP or S6A-NEP were biotinylated, and the amount of biotinylated neprilysin was evaluated by a pull-down assay. Data represent the mean ± S.D. ($n = 3$). ***, $p < 0.01$ compared with WT-NEP. *G*, Aβ levels in the conditioned medium from SH-SY5Y cells transiently expressing WT-NEP or S6A-NEP. Data represent the mean ± S.D. ($n = 4$). **, $p < 0.01$ compared with WT-NEP. *H*, neprilysin activity in whole-cell lysates from WT-NEP and S6A-NEP transfectants was measured. Data represent the mean ± S.D. ($n = 3$). *I*, the effect of NT-3 on cell surface S6A-NEP activity. SH-SY5Y cells transiently expressing S6A-NEP were treated with NT-3 for 24 h. Cell surface neprilysin activity was measured using suc-Ala-Ala-Phe-MCA substrate. Data represent the mean ± S.D. ($n = 3$).

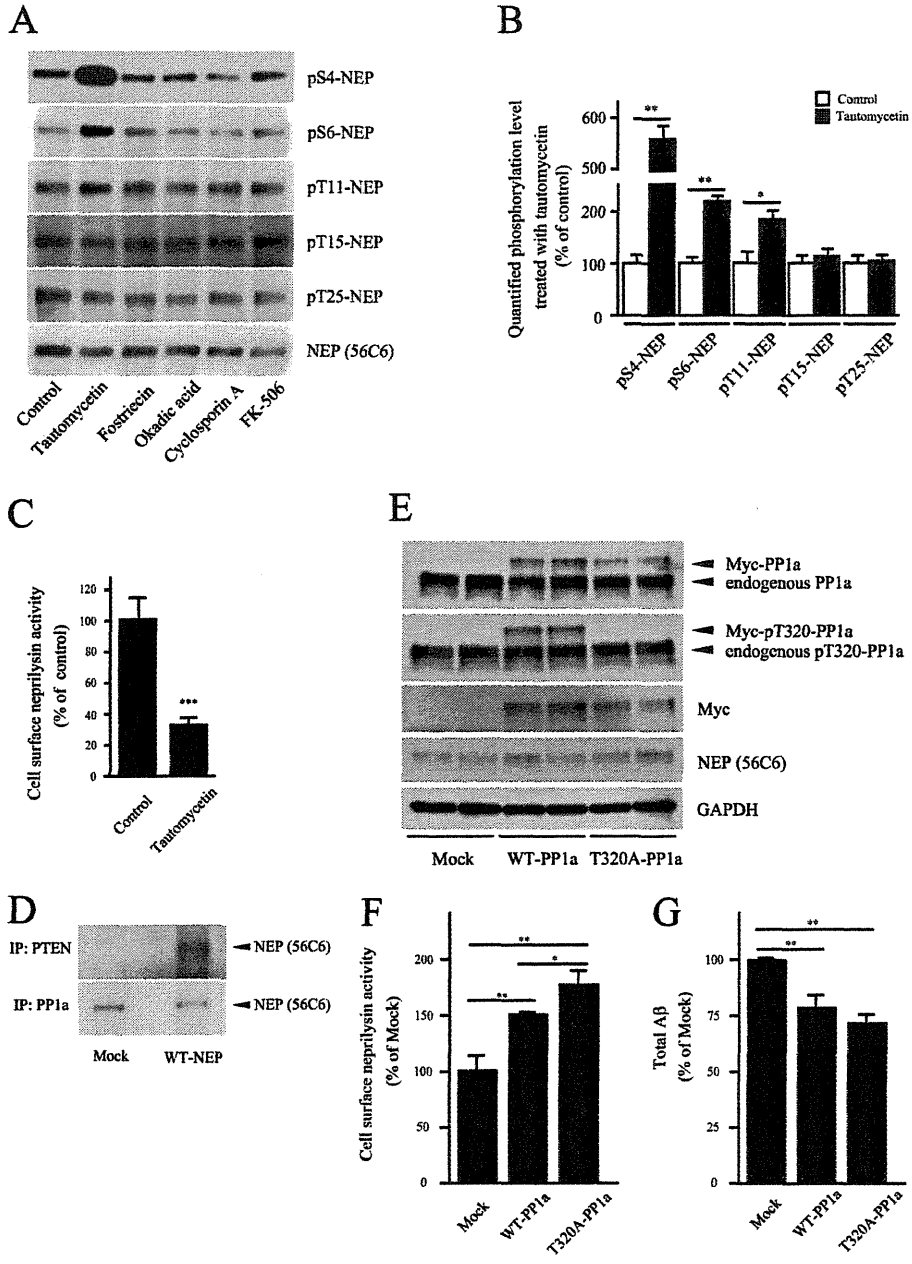

FIGURE 6. **PP1a regulates neprilysin activity through dephosphorylation.** *A*, primary neurons infected with SFV-hNEP were treated with specific inhibitors of serine/threonine phosphatases, tautomycetin (1 μM), fostriecin (100 nM), okadaic acid (10 nM), cyclosporin A (1 μM), and FK-506 (1 μM), and the phosphorylation state of neprilysin was measured by immunoprecipitation using a neprilysin antibody and immunoblot with phosphospecific antibodies. *B*, densitometric quantification of phosphorylation levels after tautomycetin treatment for 24 h as analyzed by Western blot in *A*. Data represent the mean ± S.D. (*error bars*) ($n = 3$). *, $p < 0.05$; **, $p < 0.01$ compared with non-treated. *C*, the effect of tautomycetin on cell surface neprilysin activity in primary neurons infected with SFV-hNEP. Data represent the mean ± S.D. ($n = 3$). **, $p < 0.01$ compared with control. *D*, immunoprecipitation (*IP*) of SH-SY5Y cell lysates with PTEN and PP1a antibodies. SH-SY5Y cells were transfected with a mock or WT-NEP expression vector. Lysates were prepared and immunoprecipitated using PTEN and PP1a antibodies as indicated. The immunoprecipitates were subjected to Western blot analysis, using anti-neprilysin antibody for detection. *E*, verification of WT- and T320A-PP1a expression in SH-SY5Y transfectants by Western blot and using antibodies as indicated to the *right*. *F*, the effect of PP1a activation on cell surface neprilysin activity. SH-SY5Y cells infected with SFV-hNEP were transfected with WT- or T320A-PP1a followed by measurement of cell surface neprilysin activity. Data represent the mean ± S.D. ($n = 4$). *, $p < 0.05$; **, $p < 0.01$ compared with control. *G*, effect of PP1a activation on Aβ levels. The Aβ levels in conditioned medium from WT- and T320A-PP1a-transfected SH-SY5Y cells, infected with SFV-hNEP, were quantified by ELISA. Data represent the mean ± S.D. ($n = 4$). **, $p < 0.01$ compared with control.

dence indicates the feasibility of a neprilysin-based approach. For example, overexpression of neprilysin leads to a decrease in Aβ load and improved memory in AD model mice. Another factor that argues in favor of a neprilysin-based treatment is the limited number of possible side effects. For example, the levels of neuropeptides in neprilysin knock-out mice are unaltered, indicating that proteases other than neprilysin are involved in their metabolism. Furthermore, neprilysin transgenic mice do not display other behavioral abnormalities (15–17, 39). However, in order to develop a neprilysin-based AD treatment, it is